

Transferable Reinforcement Learning via Generalized Occupancy Models

Chuning Zhu¹ Xinqi Wang¹ Tyler Han¹ Simon S. Du¹ Abhishek Gupta¹

Abstract

Intelligent agents must be generalists - showing the ability to quickly adapt and generalize to varying tasks. Within the framework of reinforcement learning (RL), model-based RL algorithms learn a task-agnostic dynamics model of the world, in principle allowing them to generalize to arbitrary rewards. However, one-step models naturally suffer from compounding errors, making them ineffective for problems with long horizons and large state spaces. In this work, we propose a novel class of models - generalized occupancy models (GOMs) - that retain the generality of model-based RL while avoiding compounding error. The key idea behind GOMs is to model the distribution of all possible long-term outcomes from a given state under the coverage of a stationary dataset, along with a policy that realizes a particular outcome from the given state. These models can then quickly be used to select the optimal action for arbitrary new tasks, without having to redo policy optimization. By directly modeling long-term outcomes, GOMs avoid compounding error while retaining generality across arbitrary reward functions. We provide a practical instantiation of GOMs using diffusion models and show its efficacy as a new class of transferable models, both theoretically and empirically across a variety of simulated robotics problems. Videos and code: <https://weirdlabuw.github.io/gom/>.

1. Introduction

Reinforcement learning agents are becoming ubiquitous in a wide array of applications, ranging from language modeling (Casper et al., 2023) to robotics (Han et al., 2023; Kober et al., 2013). Traditionally, reinforcement learning has focused on the single-task setting, where the goal is to

¹Paul G. Allen School of Computer Science and Engineering, University of Washington, Seattle, WA, USA. Correspondence to: Chuning Zhu <zchuning@cs.washington.edu>.

learn behavior that maximizes a specific reward function. However, for practical deployment, reinforcement learning agents must be able to generalize across different tasks in an environment. For instance, a mobile manipulator deployed in a home setting should not be limited to proficiency in a single task such as object relocation, but should exhibit versatile behavior that can generalize to various objects, tasks, start positions, target locations, and path preferences. In this work, we study the problem of developing reinforcement learning agents that generalize broadly to *any* task in an environment specified by a reward function.

The concept of “world models” or model-based reinforcement learning has emerged as an appealing approach for developing these types of generalist agents (Xu et al., 2022; Hafner et al., 2021; Young et al., 2023). Model-based reinforcement learning learns an approximate dynamics model in a reward-agnostic manner, which can then be used to “plan” for approximately optimal behavior for *any* downstream reward function (Sutton, 1991; Williams et al., 2017; Nagabandi et al., 2019; Rybkin et al., 2021). Typical downstream planning techniques use the dynamics model as a proxy environment, generating data autoregressively — conditioning each step on the generation from the previous step — to determine actions that approximately maximize the rewards.

A common approach to model-based RL is through one-step dynamics models trained to predict the next state from the current state and action using standard supervised learning techniques (Williams et al., 2017; Nagabandi et al., 2018; Janner et al., 2019). While this paradigm conceptually enjoys the benefit of generalization across reward functions, model-based RL algorithms relying on one-step models suffer from a critical flaw — they are prone to compounding error (Lambert et al., 2022; Asadi et al., 2018; Janner et al., 2019). Compounding error arises where small one-step approximation errors accumulate over long horizons during autoregressive generation. This leads to trajectories that vastly diverge from real trajectories, limiting most model-based RL methods to short-horizon, low-dimensional problems despite their conceptual generalization benefits. While learning objectives that directly consider multi-step dynamics propagation have been proposed (Janner et al., 2020), these often present a non-convex, challenging optimization landscape. These challenges make model-based

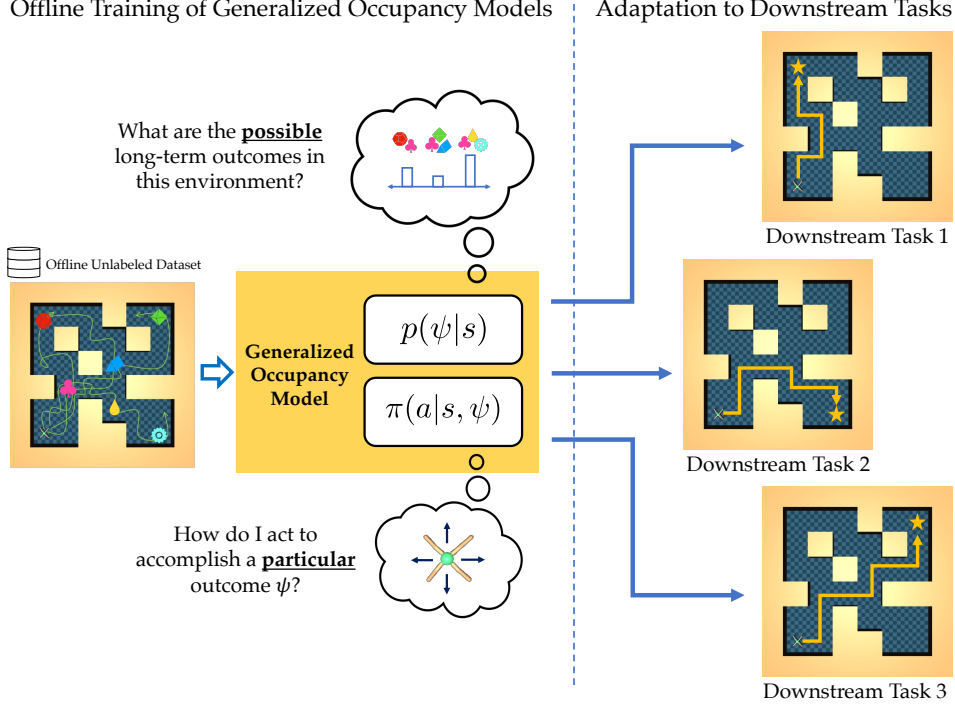


Figure 1. Depiction of the transfer setting for generalized occupancy models. Given an unlabeled offline dataset, we learn a generalized occupancy model that models both “what can happen?” $p(\psi|s)$ and “how to achieve a particular outcome?” $p(a|s, \psi)$. This is used for quick adaptation to new downstream tasks without re-planning or test-time policy optimization.

reinforcement learning an impractical choice for performant *and* transferable decision making.

An alternative approach, off-policy model-free RL (Watkins & Dayan, 1992; Konda, 2002), leverages principles of dynamic programming to directly learn the optimal policy for a *particular* reward function. These methods model the value function V_r^π (or Q-function Q_r^π), which is the expected *accumulated* rewards in the future when acting according to a particular policy π . Since there is no autoregressive generation of states, model-free RL circumvents the compounding error challenges, making them an appealing choice for building performant single-task decision-making agents (Hessel et al., 2018; Wurman et al., 2022). However, they only learn optimal policies for a single reward function, limiting application to transferable, generalist decision-making.

In this work, we leverage ideas from model-free RL to develop a new class of models — generalized occupancy models (GOMs), that avoid compounding errors while also being transferable across arbitrary reward functions. GOMs build on the off-policy model-free RL framework, but remove their dependence on a particular reward and policy, thereby enabling transfer across tasks without compounding error. At the heart of GOMs are two concepts - (1) *cumulative feature modeling*: rather than modeling the accumulation of a single reward function like off-policy RL, GOMs model the accumulation of vector-valued features $g(s)$ of states;

(2) *all-path modeling*: rather than modeling the expected accumulated feature under a single policy, GOMs model the distribution of cumulative features under *all* possible policies covered in the off-policy dataset. Condition (1) allows for *reward-agnostic* modeling of long-term environmental dynamics, while condition (2) allows for *policy-agnostic* modeling of long-term outcomes in the environment.

Concretely, GOMs model the environment dynamics by learning a distribution over all possible future “outcomes” from any given state subject to the dynamics and dataset coverage, where the outcomes are represented as cumulative features $\psi = \sum_t \gamma^{t-1} g(s_t)$. In an approximate sense, GOMs learn a model of “affordances” in the environment (Hasanin et al., 2022; Weld, 1989). The distribution over outcomes $p(\psi|s)$ is then paired with a readout policy $\pi(a|s, \psi)$ to actualize a desired outcome into a corresponding action that will accomplish this outcome.

How can we use GOMs to develop generalist agents? Given a GOM - $(p(\psi|s), \pi(a|s, \psi))$ learned in an environment, an arbitrary reward function can be maximized by noting that if rewards are *linear* in the above-mentioned (non-linear) features $g(s)$, the resulting value functions are linear in the corresponding cumulative feature ψ . As a result, through a simple linear regression procedure, we show quick adaptation to arbitrary new tasks without any test time policy optimization, planning, or dynamic programming. This en-

ables GOM to capture *any* possible task in the environment without the challenges of compounding error. We instantiate a practical algorithm for learning GOMs using diffusion models, analyze its theoretical properties, and show its efficacy on challenging decision making tasks in simulation.

2. Related Work

Our work has connections to prior work on multi-task RL and model-based reinforcement learning.

Multi-Task RL The setting of GOMs is related to multi-task RL (Varghese & Mahmoud, 2020; Kirk et al., 2023). Typical methods for multi-task generalization either condition models or policies on task descriptors (Hausman et al., 2018; Reed et al., 2022; Yu et al., 2020a; Sodhani et al., 2021; Brohan et al., 2023) or quickly finetune policies across tasks (Octo Model Team et al., 2023; Julian et al., 2020; Zhao et al., 2022; Rusu et al., 2016; Taïga et al., 2023). Conditioning methods require a known, detailed task descriptor, a challenging problem in many cases. They are also particularly susceptible to distribution shifts across training and test tasks. Finetuning methods rely on the transfer of neural network weights (Julian et al., 2020; Rusu et al., 2016), subject to the pathologies of neural dynamics. GOMs are able to *provably* generalize to any task by implicitly modeling the dynamics, without relying on brute force generalization or neural dynamics.

Successor Features A related line of work is successor features (Barreto et al., 2017; Borsa et al., 2019; Touati & Ollivier, 2021b; Chen et al., 2023; Janner et al., 2020). Similar to GOMs, they achieve generalization across various rewards by modeling the accumulation of features and reducing transfer to a linear regression problem. The key difference lies in the subtleties of policy dependence. While successor features are modeled with an implicit dependence on a *particular* policy π , GOMs model *all* possible outcomes, making them policy agnostic. Doing so allows for generalization to arbitrary new rewards *and* policies. Most closely related to our work is (Chen et al., 2023), which accomplishes policy generalization of successor features by conditioning on an open loop sequence of actions. In contrast, GOMs avoid policy conditioning by modeling the distribution of *all* possible outcomes.

Model-Based RL model-based RL aims to learn one (or multi) step dynamics models via supervised learning and use the them for planning (Chua et al., 2018; Nagabandi et al., 2018; 2019; Williams et al., 2017) or policy optimization (Deisenroth & Rasmussen, 2011; Sutton, 1991; Janner et al., 2019; Yu et al., 2020b; Hafner et al., 2020) across tasks. While improvements have been made to model architectures (Hafner et al., 2020; Janner et al., 2022; Asadi et al., 2018; Lambert et al., 2021; Zhang et al., 2021), these

methods suffer from the challenge of compounding error, where autoregressive generation can lead to large errors in predictions over long horizons (Asadi et al., 2018; Lambert et al., 2022). Rather than improving the modeling architectures, GOMs directly model long-term outcomes in an environment, avoiding step-by-step modeling and thereby compounding error.

3. Preliminaries

We adopt the standard Markov Decision Process (MDP) notation and formalism (Howard, 1960) for an MDP $\mathcal{M} = (\mathcal{S}, \mathcal{A}, r, \gamma, \mathcal{T}, \rho_0)$, but restrict our consideration to the class of deterministic (but non-countable) MDPs. While this does not encompass every environment, it does capture a significant set of problems of practical interest. Hereafter, we refer to a deterministic MDP and a *task* interchangeably. In our setting, we consider transfer across different MDPs that always share the same action space \mathcal{A} , state space \mathcal{S} , and transition dynamics $\mathcal{T} : \mathcal{S} \times \mathcal{A} \rightarrow \mathcal{S}$ ¹ The difference between tasks only lies in having different state-dependent Markovian reward functions $r : \mathcal{S} \rightarrow [0, 1]$.

Value function estimation Given a deterministic MDP \mathcal{M} , and a trajectory $\{s_i, a_i\}_{i=1}^\infty$, the cumulative reward R is defined as $R = \sum_{i=1}^\infty \gamma^{t-1} r(s_t)$. One can then define the value function under policy π as $V^\pi(s) := \mathbb{E}_{\substack{a_t \sim \pi(\cdot|s_t) \\ s_{t+1} \sim \mathcal{T}(\cdot|s_t, a_t)}} [R | s_1 = s]$, and the state-action Q-function as $Q^\pi(s, a) := \mathbb{E}_{\substack{a_t \sim \pi(\cdot|s_t) \\ s_{t+1} \sim \mathcal{T}(\cdot|s_t, a_t)}} [R | s_1 = s, a_1 = a]$. The value function admits a temporal structure that allows it to be estimated using dynamic programming, which iteratively applies the Bellman operator until a fixed point is reached $V^\pi(s) := r(s) + \gamma \mathbb{E}_\pi [V^\pi(s_2) | s_1 = s]$. While these Bellman updates are in the tabular setting, equivalent function approximator variants (e.g., with neural networks) can be instantiated to minimize an analogous Bellman “error” with stochastic optimization techniques (Mnih et al., 2013; Haarnoja et al., 2018; Mnih et al., 2016).

Problem setting We consider a transfer learning scenario where we have access to an offline dataset consisting of transition tuples $\mathcal{D} = \{(s_i, a_i, s'_i)\}_{i=0}^N$ all collected under the same dynamics \mathcal{T} . We use π_β to denote the behavior policy that generates \mathcal{D} , which can be a mixture of multiple policies. This setting resembles that of offline RL (Levine et al., 2020), with the crucial distinction that offline RL datasets typically come labeled with *task-specific* rewards. In contrast, our goal is to learn reusable knowledge from the *unlabeled* offline dataset in order to quickly adapt to any downstream tasks in the same environment. The downstream tasks can be specified in the form of a reward

¹For simplicity, we also use $\mathcal{T}(s, a)$ to denote the next state.

function or a small number of (s, r) samples. In this sense, the problem setting being considered here is one of “unsupervised reinforcement learning”. While we can formally measure the regret of learning in new tasks, the problem setting we describe will attempt to eschew exploration for the sake of zero-shot transfer to new problems².

4. Generalized Occupancy Models: All-Task Reinforcement Learning without Compounding Error

In this section, we introduce the framework of Generalized Occupancy Models (GOMs) as a scalable alternative to model-based RL for the unsupervised reinforcement learning problem described in Section 3. GOMs retain the benefits of multi-reward transfer across *all* possible tasks, without accruing compounding error in the process. We start by describing the technical details behind learning GOMs in Section 4.1, followed by a practical algorithm to train GOMs efficiently with modern tools in Section 4.2. Finally, we describe how GOMs can be used for efficient multi-task transfer in Section 4.3.

4.1. Learning Generalized Occupancy Models

To describe GOMs, let us consider a running example shown in Fig 2. In this example, we will consider an agent that must navigate around a graph consisting of 4 states $\{s_i\}_{i=0}^3$ and two actions $\{a_i\}_{i=0}^1$, taking various actions to traverse graph edges. The offline dataset consists of 4 transitions. $\mathcal{D} = \{(s_0, a_0, s_1), (s_1, a_0, s_3), (s_0, a_1, s_2), (s_2, a_0, s_3)\}$ tuples, as set up in Section 3. We set $\gamma = 1$ for simplicity.

To transfer and obtain optimal policies across arbitrary rewards, generalist decision making agents must model the future in a way that is *policy and reward agnostic* while avoiding compounding error (as in model-based RL). To this end, generalized occupancy models (GOMs) adopt an off-policy dynamic programming based technique to directly model cumulative outcomes in the future, but do so without depending on either a particular reward function $r(\cdot)$ or any particular policy π .

GOMs rely on two key principles: **(1) Reward-agnostic cumulative feature modeling:** rather than predicting immediate future outcomes like model-based RL, we model the discounted *sum* over the future $\psi = \sum_{t=1}^{\infty} \gamma^{t-1} g(s_t)$ of arbitrary cumulants $g(s)$ e.g., random features of state. While modeling discounted sums is inherent to off-policy model-free RL, in GOMs we model the discounted sum of arbitrary cumulants $g(s)$, allowing them to share future outcome predictions across rewards. Throughout this section we will refer to ψ as summed cumulants, outcomes, or affordances

²Only requiring labeled samples for reward

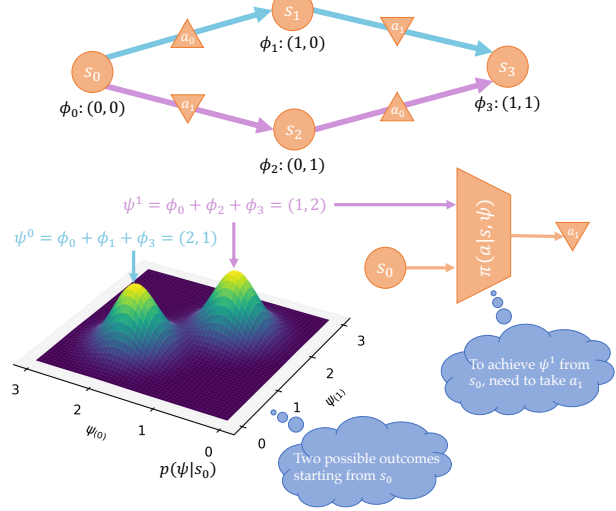


Figure 2. Depiction of all-path cumulant modeling for a simple MDP with GOMs. GOMs learn a distribution of all possible long-term outcomes (summed up cumulants ψ) as $p(\psi|s)$ along with a readout policy $\pi(a|s, \psi)$ that takes an action a to realise ψ starting at state s .

interchangeably. **(2) Policy-agnostic all-paths cumulative modeling:** rather than modeling the summed cumulants ψ under any one policy π as in off-policy RL (Q^π), we model the distribution of *all* possible outcomes $p(\psi|s)$ in the environment subject to dataset coverage. Doing so allows the outcome model to be *policy agnostic*, enabling the synthesis of optimal policies for arbitrary new tasks.

We first instantiate the framework of generalized occupancy models with an abstract cumulant $g(s)$ (as is also described in (Sutton et al., 2011; Barreto et al., 2017)) to illustrate the mechanism for policy-agnostic, all-paths cumulative modeling $p(\phi|s)$ of future outcomes ϕ , in Section 4.1.1. We then propose a particular choice of cumulant $g(s)$ that ensures that the resulting GOM is both *reward* and *policy* agnostic in Section 4.1.2. In doing so the resulting framework can easily be applied to arbitrary new tasks, naturally enabling transferability.

4.1.1. MODELING ALL-PATH CUMULANTS WITH DYNAMIC PROGRAMMING

Value functions V^π in off-policy RL model the future by accumulating a particular reward function $r(s)$ when acting according to a particular policy π . Instead of modeling the accumulation of a particular reward, let us consider modeling the accumulation of an arbitrary (vector-valued) cumulant $g : \mathcal{S} \rightarrow \mathcal{R}^k$, which is a user-defined mapping from the state of the system to a vector space \mathcal{R}^k (for instance, reward is a special case of a cumulant, with $k = 1$, and we use random Fourier features as cumulants in our experiments). For any such cumulant, GOMs aim to model the

entire **distribution** $p(\psi|s)$ of all possible future discounted sum of cumulants $\psi = \sum_{t=1}^{\infty} \gamma^{t-1} g(s_t)$ that are covered in the dataset.³ For instance, in Fig 2, starting from the state s_0 leads to the outcomes $\psi^0 = g(s_0) + g(s_1) + g(s_3)$ or $\psi^1 = g(s_0) + g(s_2) + g(s_3)$, and a GOM will aim to model a distribution over *both* of these outcomes. Modeling the sum of cumulants rather than rewards allows for transfer across rewards, while modeling *all paths* allows for transfer across policies. In addition to modeling the future outcomes under all possible paths from a state $p(\psi|s)$, GOMs pair this with a readout policy $\pi(a|s, \psi)$ which actualizes a desired long-term outcome ψ into the action a to be taken at state s to accomplish the particular long-term outcome.

As in off-policy RL, the affordance distribution $p(\psi|s)$ in GOMs can be learned via an approximate dynamic programming update which shares similarity with a distributional Bellman update:

$$\begin{aligned} \max_{\theta} \mathbb{E}_{(s, a, s') \sim \mathcal{D}} [\log p_{\theta}(g(s) + \gamma \psi_{s'}|s)] \\ \text{s.t.} \quad \psi_{s'} \sim p_{\theta}(\cdot|s') \end{aligned} \quad (1) \quad (2)$$

Intuitively, this update suggests that the distribution $(p_{\theta}(\psi|s))$ over ψ at a particular state s maximizes likelihood over cumulant $g(s)$ at the current state added to outcomes sampled from future states $\psi_{s'}$, thereby instantiating a fixed-point procedure, much like a Bellman update.

Along with the outcome distribution $p_{\theta}(\psi|s)$, the readout policy $\pi_{\theta}(a|s, \psi)$ can be obtained via maximum-likelihood estimation:

$$\begin{aligned} \max_{\theta} \mathbb{E}_{(s, a, s') \sim \mathcal{D}} [\log \pi_{\theta}(a|s, \psi = g(s) + \gamma \psi_{s'})] \\ \text{s.t.} \quad \psi_{s'} \sim p_{\theta}(\cdot|s') \end{aligned} \quad (3)$$

This update says that if an action a at a state s leads to a next state s' , then the action a should be taken with high likelihood, for outcomes ψ that are a combination of the current cumulant $g(s)$ and outcomes from the next state $\psi_{s'} \sim p_{\theta}(\cdot|s')$.

This is made clear by considering the running example described above and in Fig. 2. Suppose we have a cumulant $g(s)$ such that $g(s_0) = (0, 0)$, $g(s_1) = (1, 0)$, $g(s_2) = (0, 1)$, $g(s_3) = (1, 1)$. Starting from s_0 , there are two distinct outcomes (s_0, s_1, s_3) and (s_0, s_2, s_3) . For each outcome, we can compute a summed cumulant (with $\gamma = 1$ for simplicity) $\psi^0 = g(s_0) + g(s_1) + g(s_3) = (2, 1)$, and $\psi^1 = g(s_0) + g(s_2) + g(s_3) = (1, 2)$. The outcome distribution at state s_0 — $p(\psi|s_0)$ will thus have two modes, at $(2, 1)$ and $(1, 2)$. The readout policy will then map $(s_0, (2, 1))$ to

³Note that while also distributional, GOMs are different from distributional RL, since the distributional element of the model is coming from the marginalization across all paths, rather than stochasticity in the policy and dynamics (Bellemare et al., 2017).

a_0 and $(s_0, (1, 2))$ to a_1 , since we need to execute action a_0 at s_0 to realize the first outcome, and action a_1 at s_0 to realize the second outcome.

Intuitively, the outcome distribution $p(\psi|s)$ can be understood as a natural analogue to a value function, but with two crucial differences - (1) it represents the accumulation of not just a single reward function but rather an arbitrary (vector valued) cumulant, (2) the value function is not specific to any particular policy, but rather represents the distribution over *all* possible cumulative outcomes covered in the dataset, for all paths in the coverage of the dataset. These two points are important because (1) will provide independence from any one particular reward, while (2) will provide independence from any particular policy.

4.1.2. MODELING ALL-REWARD CUMULANTS WITH LINEAR REWARD FEATURES

All-paths modeling, as described in Section 4.1.1, obtains an affordance distribution $p_{\theta}(\psi|s)$ of possible long-term outcomes in the environment and a corresponding readout policy $\pi(a|s, \psi)$, which connects any desired outcome ψ to actions in the environment. The question becomes - *how do we go from modeling summed cumulant distributions $p(\psi|s)$ to being able to quickly obtain optimal policies for arbitrary reward functions?*

The key idea we will leverage is choosing cumulants $g(s)$ such that downstream rewards $r(s)$ can be expressed as **linear** functions of cumulants $g(s)$ (that themselves are potentially non-linear functions of s). For an expressive set of random non-linear features, any non-linear reward function can be expressed as a linear combination of these features, a common assumption in a number of prior work (Rahimi & Recht, 2007; 2008; Zhang et al., 2022; Wagenmaker et al., 2023; Chen et al., 2023; Barreto et al., 2017). Using the linearity of summation, this choice of cumulant will allow us to transform a distribution over cumulative “outcomes” $p(\psi|s)$ to a distribution over possible cumulative reward $p(R|s)$ starting from a particular state s . The ψ corresponding to the maximal possible (in-support) cumulative reward can be used to select an appropriate action using the readout policy, quickly obtaining the optimal policy *without* having to do any explicit test-time policy optimization.

Formally, assume that a cumulant $g(s)$ can be chosen such that for any reward function $r(s)$, there exists a w_r such that $r(s) = w_r^T g(s)$ for all s . Using the linearity of summation, for a summed cumulant along a particular path $\psi = \sum_{t=1}^{\infty} \gamma^{t-1} g(s_t)$, the corresponding cumulative reward $R = \sum_{t=1}^{\infty} \gamma^{t-1} r(s_t)$ can be expressed as $R = w_r^T \psi$. This suggests that the distribution of affordances $p(\psi|s)$ can be naturally converted to a distribution of cumulative rewards $p(R|s)$ given a linear projection. Note that the “distribution” over possible cumulative future rewards from a

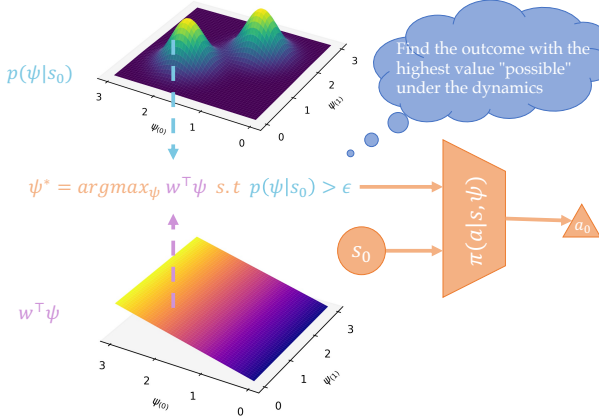


Figure 3. Depiction of planning with GOMs. Once a GOM is learned, the optimal action can be obtained by performing reward regression and searching for the optimal outcome possible under the dynamics to be decoded by the readout policy.

state $p(R|s)$ arises from the fact that we are modeling the return along all possible paths, rather than the stochasticity of policy and dynamics. As we discuss next, this distribution over returns can be used to obtain the *optimal* policy for any reward function.

4.2. Practical Instantiation

We provide an instantiation of GOMs that is used throughout our experiments. We choose the cumulant $g(s)$ to be k -dimensional random Fourier feature (Tancik et al., 2020) parameterized by a randomly initialized neural network with sine and cosine final activations (Chen et al., 2023). We parametrize both the outcome model $p(\psi|s)$ and the readout policy $\pi(a|s, \psi)$ using a conditional diffusion model (Ho et al., 2020; Song et al., 2022), although in principle any expressive generative model could be used in its place. Interestingly, as we will show in Section 4.3, the use of a diffusion model for $\nabla_\psi \log p_\theta(\psi|s)$ will allow for efficient downstream planning. We train these models (optimize Equation 2, 3) by score matching, which is a surrogate of maximum likelihood training (Song et al., 2021).

4.3. Planning and Adaptation with Generalized Occupancy Measures

To synthesize optimal policies for novel downstream reward functions, two sub-problems must be solved - (1) inferring the suitable w_r for a particular reward function from a set of (s, r) tuples, and (2) using the inferred w_r for selecting an optimal action a^* at a state s . We detail the solution to each subproblem below.

Inferring task-specific weights with linear regression

As discussed above, for any reward function $r(s, a)$, if w_r is known, then the distribution over possible future cu-

mulative rewards in the dataset $p(R|s)$ is known through linearity. However, in most cases, rewards are not provided in functional form, making w_r unknown apriori. Instead, given a dataset of $\mathcal{D} = \{(s, r)\}$ tuples, the w_r can be obtained by solving a simple linear regression problem $\text{minimize } \frac{1}{|\mathcal{D}|} \sum_{(s, r) \in \mathcal{D}} \|r - w_r^T g(s)\|_2^2$. We do not need to run an expensive policy optimization (Janner et al., 2019) or planning (Chua et al., 2018) procedure at test time, simply perform a simple linear regression procedure.

Generating task-specific policies with guided diffusion

Given the inferred w_r , and the corresponding future return distribution $p(R|s)$ obtained through linear scaling of $p(\psi|s)$, the optimal action can be obtained by finding the ψ corresponding to the highest possible future return that has sufficient data-support:

$$\max_{\psi} \quad w_r^T \psi, \quad \text{s.t. } p(\psi|s) \geq \epsilon$$

where $\epsilon > 0$ is a tuning parameter to ensure sufficient coverage for ψ . This suggests that the optimal outcome ψ is one that provides the highest future sum of rewards $w_r^T \psi$, under a particular w_r , while also a valid future outcome under the system dynamics and dataset coverage. Fig. 3 provides an illustration of the planning procedure.

This optimization problem can be solved in a number of ways. First and foremost, a standard random shooting (Tedrake, 2023) technique can be employed to sample a set of ψ from $p(\psi|s)$ and simply choose one with the highest $w_r^T \psi$. The optimality of ψ improves as the number of samples increases. Specifically, let τ denote the sampling optimality, we expect a top τ sampled ψ from $O(\frac{1}{\tau})$ samples, i.e. $\mathbb{P}_{\pi_\beta}[w_r^T \psi \leq \sum_t \gamma^{t-1} r(s_t)] \leq \tau$, where π_β denotes the behavior policy induced by the dataset. In Sec. 5 we base our theoretical analysis on this planning method.

However, the special structure of this optimization problem allows for a simple variant of guided diffusion (Dhariwal & Nichol, 2021; Janner et al., 2022) to be employed for task-directed planning when $\nabla_\psi \log p(\psi|s)$ is parameterized using a diffusion model. In particular, taking the log of the both sides of the constraint and recasting the constrained optimization via the penalty method, we get a penalized objective $\mathcal{L} = w_r^T \psi + \alpha(\log p(\psi|s) - \log \epsilon)$. Taking the gradient yields $\nabla_\psi \mathcal{L}(\psi, \alpha) = w_r + \alpha \nabla_\psi \log p(\psi|s)$. The expression for $\nabla_\psi \mathcal{L}(\psi, \alpha)$ is simply the score function $\nabla_\psi \log p(\psi|s)$ modeled during standard diffusion training in Section 4.1.1, with an added guidance term w_r . Planning then becomes a process of doing stochastic gradient Langevin dynamics (SGLD) (Welling & Teh, 2011) to obtain an optimal sample for ψ^* , using $\nabla_\psi \mathcal{L}(\psi, \alpha)$ as the gradient. In App. B we provide an alternative derivation for the planning procedure via guided diffusion, from the perspective of control as inference.

Once ψ^* has been obtained, whether through random shooting or guided diffusion, the action to execute in the environment can be obtained by inference through the readout policy $\pi_\rho(a|s, \psi^*)$. We refer the reader to Alg. 5 for a complete overview of the proposed algorithm. The significance of GOMs as described is that they allow for extremely quick transfer to arbitrary new rewards in an environment, without accumulating compounding error and without requiring a expensive test-time dynamic programming procedure. In this way, GOMs can be thought of as a new class of models of transition dynamics that avoid the typical challenges of compounding error in MBRL.

5. Theoretical Analyses of GOMs

In this section, we theoretically analyze GOMs.

5.1. Error Analysis of GOMs

We conduct a standard error analysis to connect error in estimating $p_0(\psi | s)$ to the suboptimality of the output policy (Szepesvári, 2010).

The most basic theoretical question for our method is how the suboptimality of the output policy relates to the estimation error. We start our analysis by assuming we have an $\epsilon > 0$ estimation error in the ground truth $p_0(\psi | s)$.

Assumption 5.1. We call the learnt distribution \hat{p} , a ϵ -good approximation if $\forall s \in \mathcal{S}, \|\hat{p}(\psi | s) - p_0(\psi | s)\|_\infty \leq \epsilon$.

Since GOMs depend on π_β , we need a definition to evaluate each (s, a) under the π_β and a given policy π .

Definition 5.2. We call a state-action pair (s, a) (δ, π_β) -good if over the randomness of π_β , $\mathbb{P}_{\pi_\beta}[Q^{\pi_\beta}(s, a) < \sum_{t=1}^{\infty} \gamma^{t-1} r(s_t) \mid s_1 = s] \leq \delta$. Furthermore, if for any $s, (s, \pi(s))$ is (δ, π_β) -good, then we call π a (δ, π_β) -good policy.

This definition gives us a metric to compare our learned policy with the behavior policy. Now, we can characterize the output policy in the sense of Definition 5.2.

Theorem 5.3 (main theorem). *For any MDP \mathcal{M} and an approximation \hat{p} satisfying Assumption 5.1, the learnt policy $\hat{\pi}$ given by the planning with random shooting and sampling optimality τ , is a $(\epsilon + \tau, \pi_\beta)$ -good policy.*

Lastly, the following corollary gives the classic suboptimality guarantee in terms of the value function under the Lipschitzness condition. This theorem shows the estimation error in $p_0(\psi | s)$ will be amplified by an $O\left(\frac{1}{1-\gamma}\right)$ which is necessary.

Corollary 5.4. *If we have λ -Lipschitzness near the optimal policy, i.e. $Q^*(s, a^*) - Q^*(s, a) \leq \lambda\delta$ when a is (δ, β) -good, the suboptimality of output policy $\hat{\pi}$ is $V_0^*(s_0) - V_0^{\hat{\pi}}(s_0) \leq \frac{\lambda}{1-\gamma}(\tau + \epsilon)$.*

5.2. Comparison with Model-Based Methods

In this subsection, we consider a concrete scenario to show the advantage of generalized occupancy models over typical model-based reinforcement learning methods. We consider the case where we have full data coverage, i.e., the dataset contains every possible transition.

Assumption 5.5. We assume that $|\mathcal{A} \times \mathcal{S}| < \infty$, and $\forall (s, a) \in \mathcal{S} \times \mathcal{A}, N(s, a, \mathcal{T}(s, a)) \geq 1$.

The following theorem shows that GOMs can output the optimal policy. The proof utilized the property of GOMs.

Theorem 5.6. *Under Assumption 5.5, in deterministic MDPs, GOM is guaranteed to identify an optimal policy.*

Next, we state a negative result about model-based methods. To establish a comparsion, we consider the standard class of consistent model-based methods. This class ensures that under Assumption 5.5, the method can learn *any* transition model if the number of data is sufficiently large.

Definition 5.7 (Consistent Model-Based Algorithms). We call an algorithm, Alg , to be consistent model-based algorithm if for some $c > 0$, \forall given MDP with transition dynamic $\mathcal{T}_0(\cdot | s, a)$, Alg produces an approximated transition dynamic $\hat{\mathcal{T}}(\cdot | s, a)$ such that

$$\lim_{N \rightarrow \infty} \mathbb{E}_{\mathcal{D}} \left[\|\mathcal{T}_0(s' | s, a) - \hat{\mathcal{T}}(s' | s, a)\|_\infty \right] = 0, \quad (4)$$

where \mathcal{D} contains at least N samples for all $(s, a) \in \mathcal{S} \times \mathcal{A}$.

Below we prove a *lower bound* showing with a finite number of data, even with full data coverage, there exists a deterministic MDP that *any* consistent-model-based algorithm *cannot* output the optimal policy.

Theorem 5.8. *For any consistent model-based algorithm, Alg , and a target maximum approximation error ϵ , there exists a MDP \mathcal{M} such that with $O(\frac{1}{\epsilon})$ samples for each valid (s, a) pair, the greedy policy $\hat{\pi}$ derived with $\hat{\mathcal{T}}$ suffers a $\Omega(\epsilon)$ suboptimality.*

Contrasting Theorem 5.6 and Theorem 5.8, we find that under the full data coverage assumption, there exists an MDP such that our method finds the *exact* optimal policy with finite data whereas any consistent model-based method suffers an ϵ suboptimality with finite $O(1/\epsilon)$ data. This example thus demonstrates a clear separation between GOMs and the consistent model-based method, that we also verify through experimental evaluation.

6. Experimental Evaluation

In our experimental evaluation, we aim to empirically answer the following questions (1) Can GOMs transfer across tasks without having to redo policy optimization? (2) Can

GOMs avoid the challenge of compounding error present in MBRL? (3) Can GOMs solve tasks with arbitrary rewards beyond goal-reaching problems? (4) Can GOMs go beyond the offline dataset, and accomplish “trajectory-stitching” to actualize outcomes that combine different trajectories?

We answer these questions through a number of experimental results in simulated robotics problems. We describe our problem setup and evaluation protocol to answer each of these questions. We defer detailed ablative analysis results to Appendix E, as well as detailed descriptions of the domains and baselines.

6.1. Problem Domains

D4RL Antmaze D4RL Antmaze (Fu et al., 2020) is a navigation domain that involves controlling an 8-DoF quadruped robot to reach some designated goal location. Each task corresponds to reaching a different goal location.

Franka Kitchen Franka Kitchen (Fu et al., 2020) is a robotics domain where the goal is to control a Franka arm to interact with items in the kitchen. Each task corresponds to interacting with a set of items, regardless of order, with sparse rewards on goal completion.

Preference Antmaze Preference Antmaze is a variant of D4RL Antmaze(Fu et al., 2020) where the goal is to reach the top right corner starting from the bottom right corner. The two tasks in this environment correspond to the two paths to reaching the goal, simulating different human preferences (non shortest-path goal reaching reward functions).

Roboverse Robotic Manipulation Roboverse (Singh et al., 2020) is a tabletop manipulation environment consisting of a robotic arm aiming to complete multi-step problems. Each task consists of two phases, and the offline dataset contains separate trajectories but not full task completion.

6.2. Baseline Comparisons

Successor Features We compare with two methods from the successor feature line of work. **SF** implements a version of successor feature with generalized policy improvement (Barreto et al., 2017). **RaMP** removes the policy dependence of SF by predicting cumulative features ψ from an initial state and an open-loop sequence of actions.

Model-Based RL We compare with two variants of model-based reinforcement learning. **MOPO** (Yu et al., 2020b) is a model-based offline RL method that learns an ensemble of dynamics model and performs actor-critic learning, while **COMBO** introduces pessimism into MOPO by training the policy using a conservative objective from (Kumar et al., 2020).

Goal-Conditioned RL Goal-conditioned RL enables adaptation to multiple downstream goals g . However, goal-

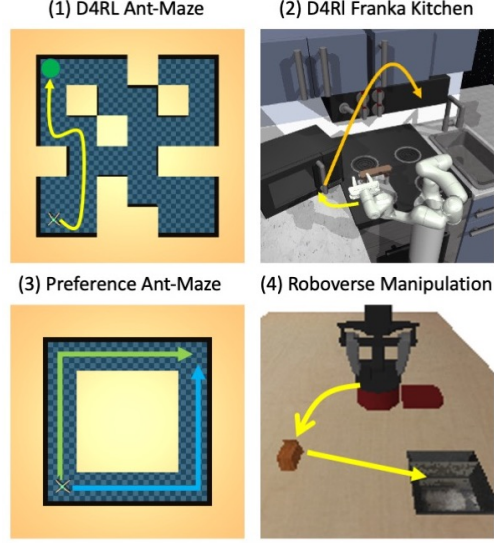


Figure 4. Evaluation Domains: (1) D4RL ant-maze (Fu et al., 2020) (2) Franka kitchen (Fu et al., 2020) (3) Preference based ant-maze with the goal of taking a particular path (4) Roboverse (Singh et al., 2020) robotic manipulation

conditioned RL is solving a more restricted class of tasks than general rewards r as goals are less expressive than rewards given the same state space. Moreover, standard GCRL is typically trained on the same set of goals as evaluation, granting them privileged information. To account for this, we consider a goal-conditioned RL baseline (**GC-IQL**) (Park et al., 2023; Kostrikov et al., 2022) and only train on goals from half the state space, to show the fragility to goal distributions. The original version trained on test-time goals is labeled **GC-IQL (Oracle)**, since it has access to privileged information.

6.3. Do GOMs learn transferable behavior across tasks?

We evaluate GOMs on transfer problems, where the dynamics are shared, but the reward functions vary. We train GOMs using the data distributions provided with the standard D4RL dataset (Fu et al., 2020). Notably, GOMs are trained once offline on this dataset and then adapted to various new tasks with simple linear regression. GOMs do not require this offline dataset to be labeled with rewards, and instead only require a small amount of reward-labeled data per downstream task to infer w_r with linear regression.

Table 1 reports the episodic return of transferring to the default D4RL tasks. GOMs are able to adapt to new tasks with just a small number of datapoints required to identify rewards via a simple linear regression, showing significantly higher transfer performance than successor features (policy dependence), model-based RL (compounding error) and goal-conditioned baselines (task-specific with goal distribution misspecification). Notably, we also find that while

Table 1. Offline multitask RL: GOMs show superior transfer performance (measured via average episodic return) than MBRL, successor features and misspecified goal conditioned baselines, while being competitive with an oracle using privileged information.

	GOM (Ours)	RaMP	SF	MOPO	COMBO	GC-IQL	GC-IQL (Oracle)
antmaze-umaze-v2	593 \pm 16	459 \pm 3	454 \pm 3	451 \pm 2	574 \pm 10	571 \pm 15	623 \pm 7
antmaze-umaze-diverse-v2	568 \pm 12	460 \pm 7	456 \pm 4	467 \pm 5	547 \pm 11	577 \pm 7	576 \pm 43
antmaze-medium-diverse-v2	631 \pm 67	266 \pm 2	238 \pm 4	236 \pm 4	418 \pm 16	403 \pm 10	659 \pm 44
antmaze-medium-play-v2	624 \pm 58	271 \pm 5	243 \pm 4	232 \pm 4	397 \pm 12	390 \pm 33	673 \pm 45
antmaze-large-diverse-v2	359 \pm 59	132 \pm 1	131 \pm 1	128 \pm 1	244 \pm 19	226 \pm 9	493 \pm 9
antmaze-large-play-v2	306 \pm 18	134 \pm 3	132 \pm 1	128 \pm 2	248 \pm 4	229 \pm 5	533 \pm 8
kitchen-partial-v0	43 \pm 6	0 \pm 0	0 \pm 0	8 \pm 7	11 \pm 9	-	33 \pm 23
kitchen-mixed-v0	46 \pm 5	0 \pm 0	0 \pm 0	0 \pm 0	0 \pm 0	-	43 \pm 7

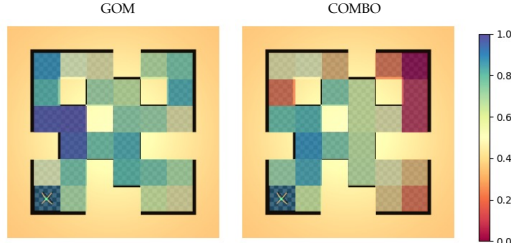


Figure 5. Transfer across tasks with GOMs and COMBO (Yu et al., 2021) in D4RL Antmaze. The visualization shows the normalized returns for reaching various goals. Each tile corresponds to a different task, navigating the robot to reach that particular tile. The color of the tile indicates the normalized return. GOMs successfully transfer across a majority of tasks, while MBRL (Yu et al., 2021) struggles on further tasks. This can be seen by the significantly higher percentage of green or blue tiles with GOMs, as compared with COMBO.

goal-conditioned RL methods have oracle information about the task and are expected to do well, GOMs are competitive in most cases with full goal coverage. The transfer ability of GOMs can also be clearly seen in Fig 5, where we plot the performance of GOMs across various different goal reaching tasks (corresponding to different tiles in the maze). We can see that GOMs have less degradation across tasks than MBRL (COMBO (Yu et al., 2021)).

6.4. Can GOMs solve tasks with *arbitrary* rewards?

While methods like goal-conditioned RL (Park et al., 2023; Ghosh et al., 2021) are restricted to shortest path goal-reaching problems, GOMs are able to solve problems with *arbitrary* reward functions. This is crucial when the reward is not easily reduced to a particular “goal”. To validate this, we evaluate GOMs on tasks with rewards simulating human preferences. These tasks are *not* simply goal-reaching problems but rather encode non-trivial human preferences in a reward function, such as particular path preferences in D4RL antmaze. In this case, we have preferences coming from dif-

Table 2. Preference learning for non-goal conditioned tasks. We see that GOMs are able to solve non-goal conditioned tasks, here taking different paths in preference ant-maze (Fig 4), while goal-conditioned RL cannot optimize for arbitrary rewards.

	GOM (Ours)	COMBO	GCSL	GC-IQL
Up		139 \pm 1	143 \pm 9	155 \pm 4
Right	142 \pm 2	136 \pm 4	20 \pm 2	83 \pm 86

ferent rewards that guide the locomotion agent specifically down the path to the left and the right, as shown in Fig 4. As we see in Table 2, GOMs and MBRL obtain policies that respect human preferences and are performant for various reward models. Goal-conditioned algorithms are unable to disambiguate preferences and simply take the shortest path to the goal. Intriguingly, we found goal-conditioned supervised learning (Ghosh et al., 2021) to consistently converge to one mode, while GC-IQL learns a high-entropy policy with some probability of taking each path.

6.5. Do GOMs perform trajectory stitching?

The ability to recover optimal behavior by combining suboptimal trajectories, or “trajectory stitching,” is crucial to off-policy RL methods as it ensures data efficiency and avoids requirements for exponential data coverage. To evaluate the ability of GOMs to perform trajectory stitching, we consider the environments introduced in (Singh et al., 2020). Here, the data only consists of trajectories that complete individual subtasks (e.g. grasping or placing), while the task of interest rewards the completion of both subtasks. Since the goal of this experiment is to evaluate stitching, not transfer, we choose the cumulants as the task rewards $g(s) = r(s)$. We find that GOMs are able to show non-trivial success rates by stitching together subtrajectories. Since RaMP (Chen et al., 2023) predicts the summed cumulants from a sequence of actions, and the optimal action sequence is not present in the dataset, it fails to solve any task. Likewise, Decision Transformer (Chen et al., 2021) does not stitch together trajectories and fails to learn meaningful behaviors.

Table 3. Evaluation of trajectory stitching ability of GOMs. GOMs are able to outperform non-stitching baselines (Decision Transformer (Chen et al., 2021)), demonstrating their abilities to recombine outcomes across trajectory segments

	GOM (Ours)	RaMP	DT
PickPlace	49 \pm 8	0 \pm 0	0 \pm 0
ClosedDrawer	40 \pm 5	0 \pm 0	0 \pm 0
BlockedDrawer	66 \pm 7	0 \pm 0	0 \pm 0

7. Discussion

In this work, we presented generalized occupancy models, a technique for modeling transition dynamics without incurring compounding error. GOMs are able to quickly adapt to provide optimal policies for *any* reward, by modeling the distribution of *all* possible future outcomes from a state in a reward and policy agnostic way. We discussed an efficient algorithm to learn GOMs and show the benefits of GOMs over standard model-based RL and off-policy RL techniques. This work has several limitations, which in turn open future directions. First, GOMs require a choice of cumulants $g(s)$ such that the rewards are linear in these cumulants. This assumption may fail, necessitating more expressive feature learning methods (Touati & Ollivier, 2021a; Nair et al., 2022). Second, the summed cumulants may alias together different trajectories, resulting in noisy action predictions. This can be mitigated by leveraging more discriminative features. Lastly, since GOMs model the behavior distribution of the dataset, the optimality of the policies is impacted by dataset skewness. This motivates the use of exploration methods for data collection.

Impact Statement

This paper presents work that aims to learn general purpose models of what is possible in an environment, and use them to quickly adapt decision making agents to new tasks. While this work is largely algorithmic in nature, and is not ready for production deployment, it may have an impact in situations where world modeling is important, such as robotics or autonomous driving. In these cases, a natural challenge with GOMs is that the interpretability that comes with autoregressive generative models is naturally lost, since only cumulative features are modeled. For future deployment of this work, we must carefully consider interpretability and think about how we can train generative heads to interpret the various outcomes that are modeled by GOMs.

References

Asadi, K., Misra, D., and Littman, M. L. Lipschitz continuity in model-based reinforcement learning. In Dy, J. G. and Krause, A. (eds.), *Proceedings of the 35th International Conference on Machine Learn-*

ing, ICML 2018, Stockholm, Sweden, July 10-15, 2018, volume 80 of Proceedings of Machine Learning Research, pp. 264–273. PMLR, 2018. URL <http://proceedings.mlr.press/v80/asadi18a.html>.

Barreto, A., Dabney, W., Munos, R., Hunt, J. J., Schaul, T., van Hasselt, H. P., and Silver, D. Successor features for transfer in reinforcement learning. *Advances in Neural Information Processing Systems*, 30, 2017.

Bellemare, M. G., Dabney, W., and Munos, R. A distributional perspective on reinforcement learning. In Precup, D. and Teh, Y. W. (eds.), *Proceedings of the 34th International Conference on Machine Learning, ICML 2017, Sydney, NSW, Australia, 6-11 August 2017, volume 70 of Proceedings of Machine Learning Research, pp. 449–458. PMLR, 2017. URL <http://proceedings.mlr.press/v70/bellemare17a.html>.*

Borsa, D., Barreto, A., Quan, J., Mankowitz, D. J., van Hasselt, H., Munos, R., Silver, D., and Schaul, T. Universal successor features approximators. In *7th International Conference on Learning Representations, ICLR 2019, New Orleans, LA, USA, May 6-9, 2019*. OpenReview.net, 2019. URL <https://openreview.net/forum?id=S1VWjiRcKX>.

Brohan, A., Brown, N., Carbajal, J., Chebotar, Y., Dabis, J., Finn, C., Gopalakrishnan, K., Hausman, K., Herzog, A., Hsu, J., Ibarz, J., Ichter, B., Irpan, A., Jackson, T., Jesmonth, S., Joshi, N. J., Julian, R., Kalashnikov, D., Kuang, Y., Leal, I., Lee, K., Levine, S., Lu, Y., Malla, U., Manjunath, D., Mordatch, I., Nachum, O., Parada, C., Peralta, J., Perez, E., Pertsch, K., Quiambao, J., Rao, K., Ryoo, M. S., Salazar, G., Sanketi, P. R., Sayed, K., Singh, J., Sontakke, S., Stone, A., Tan, C., Tran, H. T., Vanhoucke, V., Vega, S., Vuong, Q., Xia, F., Xiao, T., Xu, P., Xu, S., Yu, T., and Zitkovich, B. RT-1: robotics transformer for real-world control at scale. In Bekris, K. E., Hauser, K., Herbert, S. L., and Yu, J. (eds.), *Robotics: Science and Systems XIX, Daegu, Republic of Korea, July 10-14, 2023*, 2023. doi: 10.15607/RSS.2023.XIX.025. URL <https://doi.org/10.15607/RSS.2023.XIX.025>.

Casper, S., Davies, X., Shi, C., Gilbert, T. K., Scheurer, J., Rando, J., Freedman, R., Korbak, T., Lindner, D., Freire, P., Wang, T., Marks, S., Ségerie, C., Carroll, M., Peng, A., Christoffersen, P. J. K., Damani, M., Slocum, S., Anwar, U., Siththaranjan, A., Nadeau, M., Michaud, E. J., Pfau, J., Krasheninnikov, D., Chen, X., Langosco, L., Hase, P., Biyik, E., Dragan, A. D., Krueger, D., Sadigh, D., and Hadfield-Menell, D. Open problems and fundamental limitations of reinforcement learning from human feedback. *CoRR*, abs/2307.15217,

2023. doi: 10.48550/ARXIV.2307.15217. URL <https://doi.org/10.48550/arXiv.2307.15217>.

Chen, B., Zhu, C., Agrawal, P., Zhang, K., and Gupta, A. Self-supervised reinforcement learning that transfers using random features. *CoRR*, abs/2305.17250, 2023. doi: 10.48550/ARXIV.2305.17250. URL <https://doi.org/10.48550/arXiv.2305.17250>.

Chen, L., Lu, K., Rajeswaran, A., Lee, K., Grover, A., Laskin, M., Abbeel, P., Srinivas, A., and Mordatch, I. Decision transformer: Reinforcement learning via sequence modeling. In Ranzato, M., Beygelzimer, A., Dauphin, Y. N., Liang, P., and Vaughan, J. W. (eds.), *Advances in Neural Information Processing Systems 34: Annual Conference on Neural Information Processing Systems 2021, NeurIPS 2021, December 6-14, 2021, virtual*, pp. 15084–15097, 2021. URL <https://proceedings.neurips.cc/paper/2021/hash/7f489f642a0ddb10272b5c31057f0663-Abstract.html>.

Chua, K., Calandra, R., McAllister, R., and Levine, S. Deep reinforcement learning in a handful of trials using probabilistic dynamics models. *CoRR*, abs/1805.12114, 2018. URL <http://arxiv.org/abs/1805.12114>.

Deisenroth, M. P. and Rasmussen, C. E. PILCO: A model-based and data-efficient approach to policy search. In Getoor, L. and Scheffer, T. (eds.), *Proceedings of the 28th International Conference on Machine Learning, ICML 2011, Bellevue, Washington, USA, June 28 - July 2, 2011*, pp. 465–472. Omnipress, 2011. URL https://icml.cc/2011/papers/323_icmlpaper.pdf.

Dhariwal, P. and Nichol, A. Q. Diffusion models beat gans on image synthesis. In Ranzato, M., Beygelzimer, A., Dauphin, Y. N., Liang, P., and Vaughan, J. W. (eds.), *Advances in Neural Information Processing Systems 34: Annual Conference on Neural Information Processing Systems 2021, NeurIPS 2021, December 6-14, 2021, virtual*, pp. 8780–8794, 2021. URL <https://proceedings.neurips.cc/paper/2021/hash/49ad23d1ec9fa4bd8d77d02681df5cfa-Abstract.html>.

Fu, J., Kumar, A., Nachum, O., Tucker, G., and Levine, S. D4RL: Datasets for deep data-driven reinforcement learning. <https://arxiv.org/abs/2004.07219>, 2020.

Ghosh, D., Gupta, A., Reddy, A., Fu, J., Devin, C. M., Eysenbach, B., and Levine, S. Learning to reach goals via iterated supervised learning. In *9th International Conference on Learning Representations, ICLR 2021, Virtual Event, Austria, May 3-7, 2021*. OpenReview.net, 2021. URL <https://openreview.net/forum?id=rALA0Xo6yNj>.

Haarnoja, T., Zhou, A., Abbeel, P., and Levine, S. Soft actor-critic: Off-policy maximum entropy deep reinforcement learning with a stochastic actor. *arXiv preprint arXiv:1801.01290*, 2018.

Hafner, D., Lillicrap, T. P., Ba, J., and Norouzi, M. Dream to control: Learning behaviors by latent imagination. In *8th International Conference on Learning Representations, ICLR 2020, Addis Ababa, Ethiopia, April 26-30, 2020*. OpenReview.net, 2020. URL <https://openreview.net/forum?id=S11OTC4tDS>.

Hafner, D., Lillicrap, T. P., Norouzi, M., and Ba, J. Mastering atari with discrete world models. In *9th International Conference on Learning Representations, ICLR 2021, Virtual Event, Austria, May 3-7, 2021*. OpenReview.net, 2021. URL <https://openreview.net/forum?id=0oabwyZbOu>.

Han, D., Mulyana, B., Stankovic, V., and Cheng, S. A survey on deep reinforcement learning algorithms for robotic manipulation. *Sensors*, 23(7):3762, 2023. doi: 10.3390/S23073762. URL <https://doi.org/10.3390/s23073762>.

Hassanin, M., Khan, S. H., and Tahtali, M. Visual affordance and function understanding: A survey. *ACM Comput. Surv.*, 54(3):47:1–47:35, 2022. doi: 10.1145/3446370. URL <https://doi.org/10.1145/3446370>.

Hausman, K., Springenberg, J. T., Wang, Z., Heess, N., and Riedmiller, M. A. Learning an embedding space for transferable robot skills. In *6th International Conference on Learning Representations, ICLR 2018, Vancouver, BC, Canada, April 30 - May 3, 2018, Conference Track Proceedings*. OpenReview.net, 2018. URL <https://openreview.net/forum?id=rk07ZXZRb>.

Hessel, M., Modayil, J., van Hasselt, H., Schaul, T., Ostrovski, G., Dabney, W., Horgan, D., Piot, B., Azar, M. G., and Silver, D. Rainbow: Combining improvements in deep reinforcement learning. In McIlraith, S. A. and Weinberger, K. Q. (eds.), *Proceedings of the Thirty-Second AAAI Conference on Artificial Intelligence, (AAAI-18), the 30th innovative Applications of Artificial Intelligence (IAAI-18), and the 8th AAAI Symposium on Educational Advances in Artificial Intelligence (EAAI-18), New Orleans, Louisiana, USA, February 2-7, 2018*, pp. 3215–3222. AAAI Press, 2018. doi: 10.1609/AAAI.V32I1.11796. URL <https://doi.org/10.1609/aaai.v32i1.11796>.

Ho, J., Jain, A., and Abbeel, P. Denoising diffusion probabilistic models, 2020.

Howard, R. A. Dynamic programming and markov processes. *John Wiley*, 1960.

Janner, M., Fu, J., Zhang, M., and Levine, S. When to trust your model: Model-based policy optimization. In Wallach, H. M., Larochelle, H., Beygelzimer, A., d’Alché-Buc, F., Fox, E. B., and Garnett, R. (eds.), *Advances in Neural Information Processing Systems 32: Annual Conference on Neural Information Processing Systems 2019, NeurIPS 2019, December 8-14, 2019, Vancouver, BC, Canada*, pp. 12498–12509, 2019. URL <https://proceedings.neurips.cc/paper/2019/hash/5faf461eff3099671ad63c6f3f094f7f-Abstract.html>.

Janner, M., Mordatch, I., and Levine, S. Gamma-models: Generative temporal difference learning for infinite-horizon prediction. In Larochelle, H., Ranzato, M., Hadsell, R., Balcan, M., and Lin, H. (eds.), *Advances in Neural Information Processing Systems 33: Annual Conference on Neural Information Processing Systems 2020, NeurIPS 2020, December 6-12, 2020, virtual*, 2020. URL <https://proceedings.neurips.cc/paper/2020/hash/12ffb0968f2f56e51a59a6beb37b2859-Abstract.html>.

Janner, M., Du, Y., Tenenbaum, J. B., and Levine, S. Planning with diffusion for flexible behavior synthesis. In Chaudhuri, K., Jegelka, S., Song, L., Szepesvári, C., Niu, G., and Sabato, S. (eds.), *International Conference on Machine Learning, ICML 2022, 17-23 July 2022, Baltimore, Maryland, USA*, volume 162 of *Proceedings of Machine Learning Research*, pp. 9902–9915. PMLR, 2022. URL <https://proceedings.mlr.press/v162/janner22a.html>.

Julian, R., Swanson, B., Sukhatme, G. S., Levine, S., Finn, C., and Hausman, K. Never stop learning: The effectiveness of fine-tuning in robotic reinforcement learning. In Kober, J., Ramos, F., and Tomlin, C. J. (eds.), *4th Conference on Robot Learning, CoRL 2020, 16-18 November 2020, Virtual Event / Cambridge, MA, USA*, volume 155 of *Proceedings of Machine Learning Research*, pp. 2120–2136. PMLR, 2020. URL <https://proceedings.mlr.press/v155/julian21a.html>.

Kirk, R., Zhang, A., Grefenstette, E., and Rocktäschel, T. A survey of zero-shot generalisation in deep reinforcement learning. *Journal of Artificial Intelligence Research*, 2023.

Kober, J., Bagnell, J. A., and Peters, J. Reinforcement learning in robotics: A survey. *Int. J. Robotics Res.*, 32(11):1238–1274, 2013. doi: 10.1177/0278364913495721. URL <https://doi.org/10.1177/0278364913495721>.

Konda, V. *Actor-critic algorithms*. PhD thesis, Massachusetts Institute of Technology, Cambridge, MA, USA, 2002. URL <https://hdl.handle.net/1721.1/8120>.

Kostrikov, I., Nair, A., and Levine, S. Offline reinforcement learning with implicit q-learning. In *International Conference on Learning Representations*, 2022. URL <https://openreview.net/forum?id=68n2s9ZJWF8>.

Kumar, A., Zhou, A., Tucker, G., and Levine, S. Conservative q-learning for offline reinforcement learning. *CoRR*, abs/2006.04779, 2020. URL <https://arxiv.org/abs/2006.04779>.

Lambert, N. O., Wilcox, A., Zhang, H., Pister, K. S. J., and Calandra, R. Learning accurate long-term dynamics for model-based reinforcement learning. In *2021 60th IEEE Conference on Decision and Control (CDC), Austin, TX, USA, December 14-17, 2021*, pp. 2880–2887. IEEE, 2021. doi: 10.1109/CDC45484.2021.9683134. URL <https://doi.org/10.1109/CDC45484.2021.9683134>.

Lambert, N. O., Pister, K. S. J., and Calandra, R. Investigating compounding prediction errors in learned dynamics models. *CoRR*, abs/2203.09637, 2022. doi: 10.48550/ARXIV.2203.09637. URL <https://doi.org/10.48550/arXiv.2203.09637>.

Levine, S. Reinforcement learning and control as probabilistic inference: Tutorial and review. *CoRR*, abs/1805.00909, 2018. URL <https://arxiv.org/abs/1805.00909>.

Levine, S., Kumar, A., Tucker, G., and Fu, J. Offline reinforcement learning: Tutorial, review, and perspectives on open problems. *CoRR*, abs/2005.01643, 2020. URL <https://arxiv.org/abs/2005.01643>.

Loshchilov, I. and Hutter, F. Decoupled weight decay regularization. In *International Conference on Learning Representations*, 2019. URL <https://openreview.net/forum?id=Bkg6RiCqY7>.

Mnih, V., Kavukcuoglu, K., Silver, D., Graves, A., Antonoglou, I., Wierstra, D., and Riedmiller, M. A. Playing atari with deep reinforcement learning. *CoRR*, abs/1312.5602, 2013. URL <https://arxiv.org/abs/1312.5602>.

Mnih, V., Badia, A. P., Mirza, M., Graves, A., Lillicrap, T. P., Harley, T., Silver, D., and Kavukcuoglu, K. Asynchronous methods for deep reinforcement learning. *CoRR*, abs/1602.01785, 2016. URL <https://arxiv.org/abs/1602.01785>.

K. Asynchronous methods for deep reinforcement learning. In Balcan, M. and Weinberger, K. Q. (eds.), *Proceedings of the 33nd International Conference on Machine Learning, ICML 2016, New York City, NY, USA, June 19-24, 2016*, volume 48 of *JMLR Workshop and Conference Proceedings*, pp. 1928–1937. JMLR.org, 2016. URL <http://proceedings.mlr.press/v48/mnihal16.html>.

Nagabandi, A., Kahn, G., Fearing, R. S., and Levine, S. Neural network dynamics for model-based deep reinforcement learning with model-free fine-tuning. In *2018 IEEE International Conference on Robotics and Automation, ICRA 2018, Brisbane, Australia, May 21-25, 2018*, pp. 7559–7566. IEEE, 2018. doi: 10.1109/ICRA.2018.8463189. URL <https://doi.org/10.1109/ICRA.2018.8463189>.

Nagabandi, A., Konolige, K., Levine, S., and Kumar, V. Deep dynamics models for learning dexterous manipulation. In Kaelbling, L. P., Kragic, D., and Sugiura, K. (eds.), *3rd Annual Conference on Robot Learning, CoRL 2019, Osaka, Japan, October 30 - November 1, 2019, Proceedings*, volume 100 of *Proceedings of Machine Learning Research*, pp. 1101–1112. PMLR, 2019. URL <http://proceedings.mlr.press/v100/nagabandi20a.html>.

Nair, S., Rajeswaran, A., Kumar, V., Finn, C., and Gupta, A. R3M: A universal visual representation for robot manipulation. In Liu, K., Kulic, D., and Ichniowski, J. (eds.), *Conference on Robot Learning, CoRL 2022, 14-18 December 2022, Auckland, New Zealand*, volume 205 of *Proceedings of Machine Learning Research*, pp. 892–909. PMLR, 2022. URL <https://proceedings.mlr.press/v205/nair23a.html>.

Octo Model Team, Ghosh, D., Walke, H., Pertsch, K., Black, K., Mees, O., Dasari, S., Hejna, J., Xu, C., Luo, J., Kreiman, T., Tan, Y., Sadigh, D., Finn, C., and Levine, S. Octo: An open-source generalist robot policy. <https://octo-models.github.io>, 2023.

Park, S., Ghosh, D., Eysenbach, B., and Levine, S. Hiql: Offline goal-conditioned rl with latent states as actions. *Advances in Neural Information Processing Systems*, 2023.

Perez, E., Strub, F., de Vries, H., Dumoulin, V., and Courville, A. C. Film: Visual reasoning with a general conditioning layer. In *AAAI*, 2018.

Rahimi, A. and Recht, B. Random features for large-scale kernel machines. *Advances in Neural Information Processing Systems*, 20, 2007.

Rahimi, A. and Recht, B. Weighted sums of random kitchen sinks: Replacing minimization with randomization in learning. *Advances in Neural Information Processing Systems*, 21, 2008.

Reed, S. E., Zolna, K., Parisotto, E., Colmenarejo, S. G., Novikov, A., Barth-Maron, G., Gimenez, M., Sulsky, Y., Kay, J., Springenberg, J. T., Eccles, T., Bruce, J., Razavi, A., Edwards, A., Heess, N., Chen, Y., Hadsell, R., Vinyals, O., Bordbar, M., and de Freitas, N. A generalist agent. *CoRR*, abs/2205.06175, 2022. doi: 10.48550/ARXIV.2205.06175. URL <https://doi.org/10.48550/arXiv.2205.06175>.

Rusu, A. A., Rabinowitz, N. C., Desjardins, G., Soyer, H., Kirkpatrick, J., Kavukcuoglu, K., Pascanu, R., and Hadsell, R. Progressive neural networks. *CoRR*, abs/1606.04671, 2016. URL <http://arxiv.org/abs/1606.04671>.

Rybkin, O., Zhu, C., Nagabandi, A., Daniilidis, K., Mordatch, I., and Levine, S. Model-based reinforcement learning via latent-space collocation. In Meila, M. and Zhang, T. (eds.), *Proceedings of the 38th International Conference on Machine Learning, ICML 2021, 18-24 July 2021, Virtual Event*, volume 139 of *Proceedings of Machine Learning Research*, pp. 9190–9201. PMLR, 2021. URL <http://proceedings.mlr.press/v139/rybkin21b.html>.

Singh, A., Yu, A., Yang, J., Zhang, J., Kumar, A., and Levine, S. Cog: Connecting new skills to past experience with offline reinforcement learning. *Preprint arXiv:2010.14500*, 2020.

Sodhani, S., Zhang, A., and Pineau, J. Multi-task reinforcement learning with context-based representations. In Meila, M. and Zhang, T. (eds.), *Proceedings of the 38th International Conference on Machine Learning, ICML 2021, 18-24 July 2021, Virtual Event*, volume 139 of *Proceedings of Machine Learning Research*, pp. 9767–9779. PMLR, 2021. URL <http://proceedings.mlr.press/v139/sodhani21a.html>.

Song, J., Meng, C., and Ermon, S. Denoising diffusion implicit models, 2022.

Song, Y., Durkan, C., Murray, I., and Ermon, S. Maximum likelihood training of score-based diffusion models. In Beygelzimer, A., Dauphin, Y., Liang, P., and Vaughan, J. W. (eds.), *Advances in Neural Information Processing Systems*, 2021. URL <https://openreview.net/forum?id=AklttWFnxS9>.

Sutton, R. S. Dyna, an integrated architecture for learning, planning, and reacting. *SIGART Bull.*, 2(4):160–163, 1991. doi: 10.1145/122344.122377. URL <https://doi.org/10.1145/122344.122377>.

Sutton, R. S., Modayil, J., Delp, M., Degris, T., Pilarski, P. M., White, A., and Precup, D. Horde: a scalable real-time architecture for learning knowledge from unsupervised sensorimotor interaction. In Sonenberg, L., Stone, P., Tumer, K., and Yolum, P. (eds.), *10th International Conference on Autonomous Agents and Multiagent Systems (AAMAS 2011), Taipei, Taiwan, May 2-6, 2011, Volume 1-3*, pp. 761–768. IFAAMAS, 2011. URL <http://portal.acm.org/citation.cfm?id=2031726&CFID=54178199&CFTOKEN=61392764>.

Szepesvári, C. *Algorithms for Reinforcement Learning*. Synthesis Lectures on Artificial Intelligence and Machine Learning. Morgan and Claypool Publishers, 2010. URL <http://dx.doi.org/10.2200/S00268ED1V01Y201005AIM009>.

Taïga, A. A., Agarwal, R., Farebrother, J., Courville, A. C., and Bellemare, M. G. Investigating multi-task pretraining and generalization in reinforcement learning. In *The Eleventh International Conference on Learning Representations, ICLR 2023, Kigali, Rwanda, May 1-5, 2023*. OpenReview.net, 2023. URL <https://openreview.net/pdf?id=sSt9fROZRO>.

Tancik, M., Srinivasan, P. P., Mildenhall, B., Fridovich-Keil, S., Raghavan, N., Singhal, U., Ramamoorthi, R., Barron, J. T., and Ng, R. Fourier features let networks learn high frequency functions in low dimensional domains. *NeurIPS*, 2020.

Tedrake, R. *Underactuated Robotics*. 2023. URL <https://underactuated.csail.mit.edu>.

Touati, A. and Ollivier, Y. Learning one representation to optimize all rewards. *Advances in Neural Information Processing Systems*, 34:13–23, 2021a.

Touati, A. and Ollivier, Y. Learning one representation to optimize all rewards. In Ranzato, M., Beygelzimer, A., Dauphin, Y. N., Liang, P., and Vaughan, J. W. (eds.), *Advances in Neural Information Processing Systems 34: Annual Conference on Neural Information Processing Systems 2021, NeurIPS 2021, December 6-14, 2021, virtual*, pp. 13–23, 2021b. URL <https://proceedings.neurips.cc/paper/2021/hash/003dd617c12d444ff9c80f717c3fa982-Abstract.html>.

Varghese, N. V. and Mahmoud, Q. A survey of multi-task deep reinforcement learning. *Electronics*, 2020.

Wagenmaker, A., Shi, G., and Jamieson, K. Optimal exploration for model-based RL in nonlinear systems. *CoRR*, abs/2306.09210, 2023. doi: 10.48550/ARXIV.2306.09210. URL <https://doi.org/10.48550/arXiv.2306.09210>.

Watkins, C. J. C. H. and Dayan, P. Technical note q-learning. *Mach. Learn.*, 8:279–292, 1992. doi: 10.1007/BF00992698. URL <https://doi.org/10.1007/BF00992698>.

Weld, D. S. Donald a. norman, the psychology of everyday things. *Artif. Intell.*, 41(1):111–114, 1989. doi: 10.1016/0004-3702(89)90083-0. URL [https://doi.org/10.1016/0004-3702\(89\)90083-0](https://doi.org/10.1016/0004-3702(89)90083-0).

Welling, M. and Teh, Y. W. Bayesian learning via stochastic gradient langevin dynamics. In Getoor, L. and Scheffer, T. (eds.), *Proceedings of the 28th International Conference on Machine Learning, ICML 2011, Bellevue, Washington, USA, June 28 - July 2, 2011*, pp. 681–688. Omnipress, 2011. URL https://icml.cc/2011/papers/398_icmlpaper.pdf.

Williams, G., Wagener, N., Goldfain, B., Drews, P., Rehg, J. M., Boots, B., and Theodorou, E. A. Information theoretic MPC for model-based reinforcement learning. In *2017 IEEE International Conference on Robotics and Automation, ICRA 2017, Singapore, Singapore, May 29 - June 3, 2017*, pp. 1714–1721. IEEE, 2017. doi: 10.1109/ICRA.2017.7989202. URL <https://doi.org/10.1109/ICRA.2017.7989202>.

Wurman, P. R., Barrett, S., Kawamoto, K., MacGlashan, J., Subramanian, K., Walsh, T. J., Capobianco, R., Devlic, A., Eckert, F., Fuchs, F., Gilpin, L., Khandelwal, P., Kompella, V., Lin, H., MacAlpine, P., Oller, D., Seno, T., Sherstan, C., Thomure, M. D., Aghabozorgi, H., Barrett, L., Douglas, R., Whitehead, D., Dürr, P., Stone, P., Spranger, M., and Kitano, H. Outracing champion gran turismo drivers with deep reinforcement learning. *Nat.*, 602(7896):223–228, 2022. doi: 10.1038/S41586-021-04357-7. URL <https://doi.org/10.1038/s41586-021-04357-7>.

Xu, Y., Parker-Holder, J., Pacchiano, A., Ball, P. J., Rybkin, O., Roberts, S., Rocktäschel, T., and Grefenstette, E. Learning general world models in a handful of reward-free deployments. In Koyejo, S., Mohamed, S., Agarwal, A., Belgrave, D., Cho, K., and Oh, A. (eds.), *Advances in Neural Information Processing Systems 35: Annual Conference on Neural Information Processing Systems 2022, NeurIPS 2022, New Orleans, LA, USA, November 28 - December 9, 2022*, 2022. URL http://papers.nips.cc/paper_files/paper/2022/hash/ab6a2c6ee757afe43882121281f6065c-Abstract-Confere.html.

Young, K. J., Ramesh, A., Kirsch, L., and Schmidhuber, J. The benefits of model-based generalization in rein-

forcement learning. In Krause, A., Brunskill, E., Cho, K., Engelhardt, B., Sabato, S., and Scarlett, J. (eds.), *International Conference on Machine Learning, ICML 2023, 23-29 July 2023, Honolulu, Hawaii, USA*, volume 202 of *Proceedings of Machine Learning Research*, pp. 40254–40276. PMLR, 2023. URL <https://proceedings.mlr.press/v202/young23a.html>.

Yu, T., Kumar, S., Gupta, A., Levine, S., Hausman, K., and Finn, C. Gradient surgery for multi-task learning. In Larochelle, H., Ranzato, M., Hadsell, R., Balcan, M., and Lin, H. (eds.), *Advances in Neural Information Processing Systems 33: Annual Conference on Neural Information Processing Systems 2020, NeurIPS 2020, December 6-12, 2020, virtual*, 2020a. URL <https://proceedings.neurips.cc/paper/2020/hash/3fe78a8acf5fda99de95303940a2420c-Abstract.html>.

Yu, T., Thomas, G., Yu, L., Ermon, S., Zou, J., Levine, S., Finn, C., and Ma, T. Mopo: Model-based offline policy optimization. *Preprint arXiv:2005.13239*, 2020b.

Yu, T., Kumar, A., Rafailov, R., Rajeswaran, A., Levine, S., and Finn, C. Combo: Conservative offline model-based policy optimization. In Ranzato, M., Beygelzimer, A., Dauphin, Y., Liang, P., and Vaughan, J. W. (eds.), *Advances in Neural Information Processing Systems*, volume 34, pp. 28954–28967. Curran Associates, Inc., 2021.

Zhang, M. R., Paine, T., Nachum, O., Paduraru, C., Tucker, G., Wang, Z., and Norouzi, M. Autoregressive dynamics models for offline policy evaluation and optimization. In *9th International Conference on Learning Representations, ICLR 2021, Virtual Event, Austria, May 3-7, 2021*. OpenReview.net, 2021. URL <https://openreview.net/forum?id=kmqjgSNXby>.

Zhang, T., Ren, T., Yang, M., Gonzalez, J., Schuurmans, D., and Dai, B. Making linear mdps practical via contrastive representation learning. In Chaudhuri, K., Jegelka, S., Song, L., Szepesvári, C., Niu, G., and Sabato, S. (eds.), *International Conference on Machine Learning, ICML 2022, 17-23 July 2022, Baltimore, Maryland, USA*, volume 162 of *Proceedings of Machine Learning Research*, pp. 26447–26466. PMLR, 2022. URL <https://proceedings.mlr.press/v162/zhang22x.html>.

Zhao, M., Abbeel, P., and James, S. On the effectiveness of fine-tuning versus meta-reinforcement learning. In Koyejo, S., Mohamed, S., Agarwal, A., Belgrave, D., Cho, K., and Oh, A. (eds.), *Advances in Neural Information Processing Systems 35: Annual Conference on Neural Information Processing Systems 2022, NeurIPS 2022, New Orleans, LA, USA, November 28 - December 9, 2022*, 2022. URL http://papers.nips.cc/paper_files/paper/2022/hash/a951f595184aec1bb885ce165b47209a-Abstract-Confere.html.

Supplementary Materials for “Transferable Reinforcement Learning via Generalized Occupancy Models”

A. Missing Proofs

In this following sections, we use $1_{\mathcal{E}}$ to denote the indicator of event \mathcal{E} .

A.1. Proof of Theorem 5.3

To state the Theorem 5.3 rigorously, we introduce the basic setting here. The cumulant at time step i , $g(s_i) \in [0, 1 - \gamma]^d$ and the outcome $\psi = \sum_{i=0}^{\infty} \gamma^i g(s_i) \in [0, 1]^d$. Also, we have a policy function π s.t. $\hat{a} \sim \hat{\pi}(s, \psi)$ always leads to a successor state s' s.t. $\hat{p}(\frac{1}{\gamma}(\psi - g(s)) \mid s') > 0$.

We simplify the planning phase of GOM into the following form: For a given reward weight w_r , in each time step, we have

1. Infer optimal outcome $\psi^* = A(s, \hat{p})$ through random shooting;
2. Get corresponding action from $\hat{\pi}$, $\hat{a} \sim \hat{\pi}(s, \psi^*)$.

where the random shooting oracle A with sampling optimality τ satisfies

$$w_r^T A(s, \hat{p}) \geq \min\{R \mid \int 1_{[w_r^T \psi \geq R]} \hat{p}[\psi \mid s] d\psi \leq \tau\}.$$

This intuitively means that there are at most probability of $\tau \in [0, 1]$ the behavior policy achieving higher reward.

Proof. It suffices to prove that $\forall s, (s, \hat{\pi}(s))$ is at least $(\tau + \epsilon, \pi_{\beta})$ -good. For simplicity, we denote $\hat{R} := \min\{R \mid \int 1_{[w_r^T \psi \geq R]} \hat{p}[\psi \mid s] d\psi \leq \tau\}$. Then

$$\begin{aligned} & \mathbb{P}_{\pi_{\beta}}[w_r^T \sum_{t=1}^{\infty} \gamma^{t-1} g(s_t) \geq Q^{\pi_{\beta}}(s, \hat{\pi}(s))] \\ &= \mathbb{P}_{\psi \sim p_0(\cdot \mid s)}[w_r^T \psi \geq w_r^T \psi^*] \\ &= \int 1_{[w_r^T \psi \geq w_r^T \psi^*]} p_0(\psi \mid s) d\psi \\ &\leq \int 1_{[w_r^T \psi \geq \hat{R}]} p_0(\psi \mid s) d\psi \\ &= \int 1_{[w_r^T \psi \geq \hat{R}]} \hat{p}(\psi \mid s) d\psi \\ &\quad + \int 1_{[w_r^T \psi \geq \hat{R}]} [p_0(\psi \mid s) - \hat{p}(\psi \mid s)] d\psi \\ &\leq \tau + \int 1_{[w_r^T \psi \geq \hat{R}]} \epsilon d\psi \\ &\leq \tau + \epsilon. \end{aligned}$$

□

A.2. Proof of Corollary 5.4

Proof. Intuitively, policy $\hat{\pi}$ fall behind by at most $\lambda(\tau + \epsilon)$ at each time step: $\forall s_1 \in S$,

$$\begin{aligned}
 & V^*(s_1) - V^{\hat{\pi}}(s_1) \\
 &= Q^*(s_1, a^*) - Q^{\hat{\pi}}(s_1, \hat{a}) \\
 &= Q^*(s_1, a^*) - Q^*(s_1, \hat{a}) \\
 &\quad + Q^*(s_1, \hat{a}) - Q^{\hat{\pi}}(s_1, \hat{a}) \\
 &\leq \lambda(\tau + \epsilon) + Q^*(s_1, \hat{a}) - Q^{\hat{\pi}}(s_1, \hat{a}) \\
 &= \lambda(\tau + \epsilon) + \gamma \mathbb{E}_{s_2 \sim p(s_1, \hat{a})} [V^*(s_2) - V^{\hat{\pi}}(s_2)] \\
 &\leq \lambda(\tau + \epsilon) + \gamma \lambda(\tau + \epsilon) \\
 &\quad + \gamma^2 \mathbb{E}_{s_3} [V^*(s_3) - V^{\hat{\pi}}(s_3)] \\
 &\leq \dots \\
 &\leq \sum_{i=0}^{\infty} \gamma(\tau + \epsilon) \\
 &= \frac{\lambda}{1 - \gamma}(\tau + \epsilon).
 \end{aligned}$$

□

A.3. Proof of Theorem 5.6

Proof. While Assumption 5.5 is clear, τ can be set to be zero for concrete actions, and condition $p(\psi|s) > \epsilon$ is replaced with $p(\psi|s) > 0$. Then we see that planning only focuses on the supporting set of \hat{p} : $\hat{p}(\psi | s) = 0$ if and only $(s, \psi) \in \mathcal{D}$ for some time during execution, which equals $p_0(\psi | s) = 0$. This indicates that $\text{supp}(\hat{p}) = \text{supp}(p_0)$. Therefore the conclusion follows. □

A.4. Proof of Theorem 5.8

Proof. Because reasonable model-based algorithms don't consider the actual reward while approximate the transition dynamics, it suffices to prove that the algorithm is destined to suffer $\Omega(\epsilon)$ error in dynamic approximation.

Specifically, consider a MDP family $M = \{\mathcal{M}_1, \mathcal{M}_2\}$, both of which have four states s_1, s_2, s_3, s_0 and two actions a_1, a_2 . Both MDPs start at s_1 . The reward function $r(\cdot)$ satisfies

$$\begin{aligned}
 r(s_1) &= 0 \\
 r(s_2) &= 1 \\
 r(s_3) &= 0 \\
 r(s_0) &= 1 - \frac{\epsilon}{2}
 \end{aligned}$$

In \mathcal{M}_1 ,

$$\begin{aligned}
 \mathcal{T}_1(\cdot | s_1, a_1) &= [0, 0, 1, 0] \\
 \mathcal{T}_1(\cdot | s_1, a_2) &= [1, 0, 0, 0] \\
 \mathcal{T}_1(s_1 | s, a) &= 1, \text{ for } s = s_0, s_2, s_3, a = a_1, a_2
 \end{aligned}$$

In \mathcal{M}_2 ,

$$\begin{aligned}
 \mathcal{T}_1(\cdot | s_1, a_1) &= [0, 0, 1 - \epsilon, \epsilon] \\
 \mathcal{T}_1(\cdot | s_1, a_2) &= [1, 0, 0, 0] \\
 \mathcal{T}_1(s_1 | s, a) &= 1, \text{ for } s = s_0, s_2, s_3, a = a_1, a_2
 \end{aligned}$$

The only difference between \mathcal{M}_1 and \mathcal{M}_2 lies in the transition from s_1 . Let π_β be the an algorithm that takes a_2 and a_1 alternatively each time it reaches s_1 , and $4N$ denote the number of total samples, so that we have N samples for (s_1, a_1) . As is shown in Figure 6, $\mathbb{E}_{s \sim \mathcal{T}_1(s_1, a_1)} [r(s)] = 1$, and $\mathbb{E}_{s \sim \mathcal{T}_1(s_1, a_1)} [r(s)] = 1 - \epsilon$, which causes a $\epsilon/2$ suboptimality for every two time steps, resulting in $\frac{\gamma}{2-2\gamma^2}\epsilon$ total suboptimality for infinite horizons.

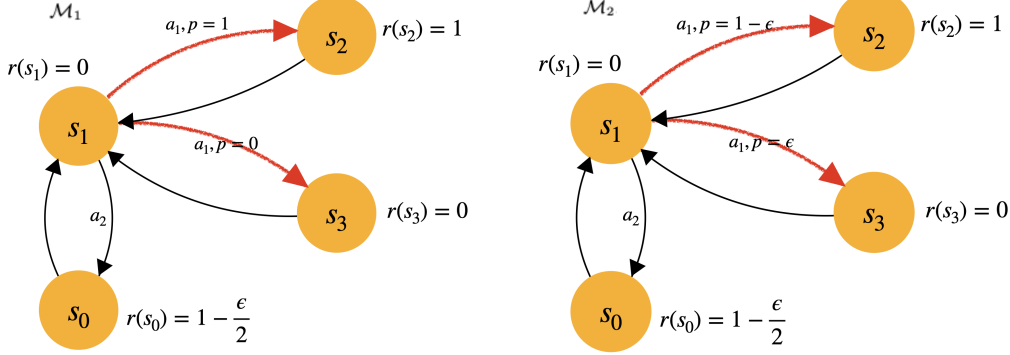


Figure 6. \mathcal{M}_1 (left) and \mathcal{M}_2 (right). The only difference lies in the transition dynamic of (s_1, a_1) , which always goes to s_2 in \mathcal{M}_1 and goes to s_3 with probability ϵ in \mathcal{M}_2 . At s_1 , optimal policy takes a_1 in \mathcal{M}_1 and a_2 in \mathcal{M}_2 . Suboptimal policies suffers a $\frac{\gamma}{2-2\gamma^2}\epsilon$ suboptimality in both MDPs.

Now, denote uniform distribution, ν over M , and the averaged error count $e_{Alg} = \mathbb{E}_{\mathcal{D}, i \sim \nu} [1_{\{\hat{\mathcal{T}} \neq \mathcal{T}_i\}}]$. Also, define the event $\mathcal{E} := \{\text{all the transitions from } s_1 \text{ goes to } s_2\}$. Here we use $i \sim \nu$ to denote that Alg is trained on \mathcal{M}_1 and \mathcal{M}_2 with equal probability.

$$\begin{aligned}
 e_{Alg} &= \mathbb{E}_{\mathcal{D}, i \sim \nu} [1_{\{\hat{\mathcal{T}} \neq \mathcal{T}_i\}}] \\
 &\geq \mathbb{P}[\mathcal{E}] \mathbb{E}_{\mathcal{D}, i \sim \nu} [1_{\{\hat{\mathcal{T}} \neq \mathcal{T}_i\}} \mid \mathcal{E}] \\
 &\geq \mathbb{P}[\mathcal{E} \cap \{i = 1\}] \mathbb{E}_{\mathcal{D}, \mathcal{M}_1} [1_{\{\hat{\mathcal{T}} \neq \mathcal{T}_1\}} \mid \mathcal{E}] + \mathbb{P}[\mathcal{E} \cap \{i = 2\}] \mathbb{E}_{\mathcal{D}, \mathcal{M}_2} [1_{\{\hat{\mathcal{T}} \neq \mathcal{T}_2\}} \mid \mathcal{E}] \\
 &= \frac{1}{2} \mathbb{E}_{\mathcal{D}, \mathcal{M}_1} [1_{\{\hat{\mathcal{T}} \neq \mathcal{T}_1\}} \mid \mathcal{E}] + \frac{(1-\epsilon)^N}{2} \mathbb{E}_{\mathcal{D}, \mathcal{M}_2} [1_{\{\hat{\mathcal{T}} \neq \mathcal{T}_2\}} \mid \mathcal{E}] \\
 &\geq \frac{(1-\epsilon)^N}{2} \mathbb{E}_{\mathcal{D}} [1_{\{\hat{\mathcal{T}} \neq \mathcal{T}_1\}} + 1_{\{\hat{\mathcal{T}} \neq \mathcal{T}_2\}} \mid \mathcal{E}] \\
 &= \frac{(1-\epsilon)^N}{2}. \tag{*}
 \end{aligned}$$

Note that $*$ is valid because the datasets conditioned on \mathcal{E} are the same for both MDPs. Because we only have two MDPs in M , and the optimal policy of one of them serves as the suboptimal one for the other, $\hat{\mathcal{T}} \neq \mathcal{T}_i$ indicates a $\frac{\gamma}{2-2\gamma^2}\epsilon$ suboptimality of output policy. Then with $N = O(1/\epsilon)$, we have

$$\begin{aligned}
 \mathbb{E}_{\mathcal{D}, i \sim \nu} [(V^{\pi^*}(s_1) - V^{\hat{\pi}}(s_1))] &= e_{Alg} \frac{\gamma}{2-2\gamma^2}\epsilon \\
 &= \frac{(1-\epsilon)^N \gamma}{4(1-\gamma^2)}\epsilon \\
 &= \Omega \left(\frac{(1-\epsilon)^{\frac{1}{\epsilon}} \gamma}{4(1-\gamma^2)} \epsilon \right) \\
 &= \Omega(\epsilon).
 \end{aligned}$$

Therefore, the averaged suboptimality over M is $\Omega\epsilon$, from which the conclusion follows. \square

B. Alternative Derivation of Guided Diffusion Planner

In this section, we derive the guided diffusion planner from the perspective of control as inference (Levine, 2018). To start, we define the trajectory-level optimality variable \mathcal{O} as a Bernoulli variable taking the value of 1 with probability $\exp(R(\tau))$ and 0 otherwise, where $R(\tau) = \sum_{t=0}^T \gamma^t r(s_t) - R_{\max}$. Note we subtract the max discounted return R_{\max} to make the density a valid probability distribution. Planning can be cast as an inference problem where the goal is to sample $\psi^* \sim p(\psi|\mathcal{O})$. By Bayes rule, we have

$$p(\psi|\mathcal{O}) \propto p(\mathcal{O}|\psi)p(\psi)$$

Taking the gradient of the log of both sides, we get

$$\begin{aligned} \nabla_{\psi} \log p(\psi|\mathcal{O}) &= \nabla_{\psi} \log p(\mathcal{O}|\psi) + \nabla_{\psi} \log p(\psi) \\ &= \nabla_{\psi} \log \exp(w^T \psi) + \nabla_{\psi} \log p(\psi) \\ &= \nabla_{\psi} w^T \psi + \nabla_{\psi} \log p(\psi) \\ &= w + \nabla_{\psi} \log p(\psi) \end{aligned}$$

This implies that we can sample from $p(\psi|\mathcal{O})$ by adding the regression weights w to the score at each timestep, yielding the same guided diffusion form as in Sec. 4.3.

C. Implementation Details

C.1. Model architecture

We parameterize the random Fourier features using a randomly initialized 2-layer MLP with 2048 units in each hidden layer, followed by sine and cosine activations. For a k -dimensional feature, the network's output dimension is $k/2$ and the final feature is a concatenation of sine and cosine activated outputs. We set $k = 128$ for all of our experiments.

We implement the outcome model and policy using conditional DDIMs (Song et al., 2022). The noise prediction network is implemented as a 1-D Unet with down dimensions [256, 512, 1024]. Each layer is modulated using FiLM (Perez et al., 2018) to enable conditioning.

C.2. Training details

For each environment, we train our model on the offline dataset for 100000 gradient steps using the AdamW optimizer (Loshchilov & Hutter, 2019) with batch size 2048. The learning rate for the outcome model and the policy are set to $3e^{-4}$ and adjusted using a cosine learning rate schedule with 500 warmup steps. We use 1000 diffusion timesteps during training and 50 timesteps for sampling with a DDIM sampler (Song et al., 2022). Sampling is conducted through an exponential moving average model with decay rate 0.995. For adaptation, we perform stochastic gradient on the regression weights w with learning rate $3e^{-4}$. **We use the same set of training hyperparameters across all environments.**

We use the guided diffusion planner on all experiments. The guidance coefficient is 0.5 for antmaze and 0.01 for kitchen, and 0.05 for Roboverse. We found planning to be quite sensitive to the guidance coefficient. Hence, for new environments, we suggest using the random shooting planner to get a baseline performance and then tuning the guided diffusion coefficient to improve performance and speed up inference. We run each experiment with 4 random seeds and report the mean and standard deviation in the tables.

C.3. Baselines

Successor Features The original successor feature method (Barreto et al., 2017) learns the policy-dependent successor feature networks for a set of policies and performs generalized policy improvement, i.e. search for the best policy among the set at test time. We implement an approximate version of SF by training a goal-conditioned policy using goal-conditioned supervised learning (Ghosh et al., 2021), along with a goal-conditioned successor feature network. At test time, we provide the algorithm a set of goals from the dataset and choose the best goal-conditioned policy to execute.

RaMP We adapt the original RaMP implementation (Chen et al., 2023) and convert it into an offline method. RaMP originally has an offline training and an online adaptation stage, where online adaptation alternates between data collection

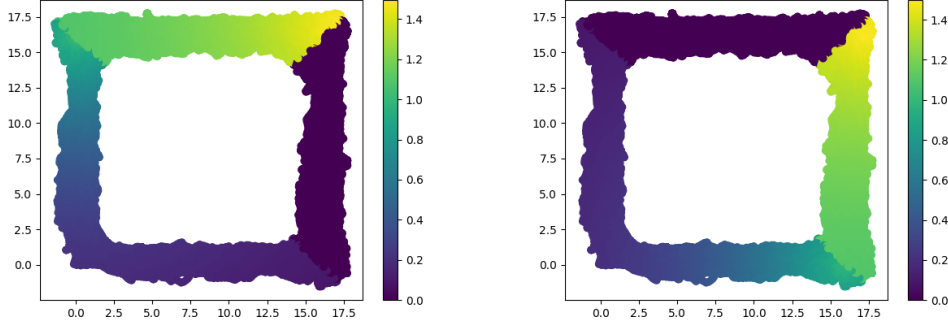


Figure 7. Data distribution and reward for Antmaze Preference environments

Table 4. Ablation of planning method. Wall time is measured over 1000 planning steps.

	Return \uparrow	Wall time (s) \downarrow
ATRL (Ours)	631 \pm 67	42.9
Random shooting @ 1000	650 \pm 50	94.8
Random shooting @ 100	619 \pm 90	58.6
Random shooting @ 10	513 \pm 52	55.5

and linear regression. We instead adapt by relabelling the offline dataset with test-time reward function, thus removing the exploration challenge. We use an MPC horizon of 15 for all experiments.

Model-based RL We use the original implementations of MOPO (Yu et al., 2020b) and COMBO (Yu et al., 2021) in our evaluations. We set the model rollout length for both methods to 5 and the CQL coefficient to be 0.5 for COMBO.

Goal-conditioned RL We use the GC-IQL baseline from (Park et al., 2023). To remove the privileged information, we modify the sampling distribution to exclude the test-time goal location.

D. Environment Details

Antmaze We use the standard offline dataset from D4RL antmaze. We replace the standard sparse reward $\mathbb{1}(s = g)$ with a dense reward $\exp(-\|s - g\|_2^2/20)$.

Franka Kitchen We use the standard offline dataset of D4RL kitchen. We use the Markovian sparse rewards for downstream task adaptation, where at each timestep the robot gets a reward equal to the number of completed tasks. For evaluation, we report the number of tasks completed throughout the entire episode.

Preference Antmaze Preference Antmaze is a variant of D4RL Antmaze(Fu et al., 2020) where the goal is to reach the top right corner starting from the bottom right corner. The two tasks in this environment correspond to the two paths to reaching the goal, simulating different human preferences (non shortest-path goal reaching reward functions). To construct the dataset, we collect 1M transitions using the D4RL waypoint controller. For each preference, we design a reward function that encourages the agent to take one path and penalize the other. Fig. 7 visualizes the dataset and the reward function for each preference.

Roboverse Robotic Manipulation Roboverse (Singh et al., 2020) is a tabletop manipulation environment consisting of a WidowX arm aiming to complete multi-step problems. Each task consists of two phases, and the offline dataset contains separate trajectories but not full task completion. We use the standard sparse reward, assigning a reward of 1 for each timestep the task is completed.

Table 5. Ablation of feature dimension and type

	Return
ATRL (Ours)	631 ± 67
Fourier features (64-dim)	561 ± 45
Fourier features (32-dim)	295 ± 30
Fourier features (16-dim)	307 ± 38
Random features (128-dim)	382 ± 43

E. Additional Experiments

To understand the impact of various design decisions on the performance of GOMs, we conducted systematic ablations on the various components, using the antmaze-medium-diverse-v2 as a test bed.

E.1. Ablation of Planning Method

We compare the guided diffusion planner with the random shooting planner as detailed in Sec. 4.3. As shown in Table 4, the guided diffusion planner achieves comparable performance to random shooting with 1000 particles while taking significantly less wall-clock time. While we can decrease the number of samples in the random shooting planner to improve planning speed, this comes at the cost of optimality.

E.2. Comparing Feature Dimension and Type

To understand the importance of feature dimension and type, we compare variants of our method that use lower-dimensional random Fourier features or plain random features parameterized by a random neural network. From Table. 5 we observe that as feature dimension decreases, their expressivity diminishes, resulting in lower performance. We found random feature to perform much worse than random Fourier features.

F. Algorithm Pseudocode

Algorithm 1 GOM Training

- 1: Given transition dataset \mathcal{D} , cumulant function $g(\cdot)$
- 2: Initialize $p_\theta(\psi|s)$, $\pi_\rho(a|s, \psi)$.
- 3: **while** not converged **do**
- 4: Draw B transition tuples $\{s_i, a_i, s'_i\}_{i=1}^B \sim \mathcal{D}$.
- 5: Sample successor features for next states $\psi'_i \sim p_\theta(\psi|s'_i)$, $i = 1 \dots N$.
- 6: Construct target successor feature $\psi_i^{\text{targ}} = g(s) + \gamma * \psi'_i$.
- 7: // ψ model learning
- 8: Update feature distribution: $\theta \leftarrow \arg \max_\theta \log p_\theta(\psi_i^{\text{targ}}|s_i)$.
- 9: // Policy extraction
- 10: Update policy: $\rho \leftarrow \arg \max_\rho \log \pi_\rho(a|s_i, \psi_i^{\text{targ}})$.
- 11: **end while**

Algorithm 2 GOM Offline Adaptation

- 1: Given transition dataset \mathcal{D} , cumulant function $g(\cdot)$, reward function $r(s)$.
- 2: Relabel offline dataset \mathcal{D} with reward function.
- 3: Initialize regression weights w .
- 4: Fit w to \mathcal{D} using linear regression $w = \arg \min_w \mathbb{E}_{\mathcal{D}}[\|w^\top g(s) - r(s)\|_2^2]$.

Algorithm 3 GOM Online Adaptation

- 1: Given $p_\theta(\psi|s)$, $\pi_\rho(a|s, \psi)$, cumulant function $g(\cdot)$.
- 2: Prefill online buffer \mathcal{D}_{buf} with random exploration policy.
- 3: Initialize regression weights w .
- 4: **for** time steps $1 \dots T$ **do**
- 5: Fit w using linear regression $w = \arg \min_w \mathbb{E}_{\mathcal{D}_{\text{buf}}} [\| w^\top g(s) - r(s) \|_2^2]$.
- 6: Infer optimal $\psi^* = \arg \max_\psi w^\top \psi$ s.t. $p_\theta(\psi|s) > \epsilon$.
- 7: Sample optimal action $a^* \sim \pi(a|s, \psi^*)$.
- 8: Execute action in the environment and add transition to buffer.
- 9: **end for**

Algorithm 4 GOM Inference (Random Shooting)

- 1: Given $p_\theta(\psi|s)$, $\pi_\rho(a|s, \psi)$, regression weight w , current state s .
- 2: Sample N outcomes $\{\psi_i\}_{i=1}^N \sim p_\theta(\psi|s)$.
- 3: Compute corresponding values $\{v_i\}_{i=1}^N$, where $v_i = w^\top \psi_i$.
- 4: Take optimal cumulant $\psi^* = \psi_i$, where $i = \arg \max_i \{v_i\}_{i=1}^N$.
- 5: Sample optimal action $a^* \sim \pi(a|s, \psi^*)$.

Algorithm 5 GOM Inference (Guided diffusion)

- 1: Given diffusion model $p_\theta(\psi|s)$, $\pi_\rho(a|s, \psi)$, regression weight w , current state s , guidance coefficient β .
- 2: Initialize outcome ψ_1 from prior.
- 3: **for** diffusion timestep $t = 1 \dots T$ **do**
- 4: Compute noise at timestep $\epsilon = \epsilon_\theta(\psi_t, t, s)$.
- 5: Update noise $\epsilon' = \epsilon - \beta \sqrt{1 - \bar{\alpha}_t} w$.
- 6: Sample next timestep action ψ_{t+1} using ϵ' .
- 7: **end for**
- 8: Sample optimal action $a^* \sim \pi_\rho(a|s, \psi_T)$.
